Phase Equilibria in the C_{60} + Ferrocene System and Solid-State Studies of the C_{60}·2Ferrocene Solvate

P. Espeau

Laboratoire de Chimie Physique, Faculté de Pharmacie, Université Paris 5, 4 avenue de l'Observatoire, 75006 Paris, France

M. Barrio, D. O. López, J. Ll. Tamarit,* and R. Céolin†

Departament de Fisica i Enginyeria Nuclear, ETSEIB, Universitat Politècnica de Catalunya, Diagonal 647, 08028 Barcelona, Catalonia, Spain

H. Allouchi and V. Agafonov

Laboratoire de Chimie Physique, Faculté de Pharmacie, Université de Tours, 31 avenue Monge, 37200 Tours, France

F. Masin

Matière condensée et Résonance magnétique CP-232, Faculté des Sciences, Université Libre de Bruxelles, Campus de la plaine, Boulevard du Triomphe, B-1050 Bruxelles, Belgique

H. Szwarc

Laboratoire de Chimie Physique, UMR 8000, Université Paris Sud - CNRS, bâtiment 490, 91405 Orsay Cedex, France

Received July 4, 2001. Revised Manuscript Received September 3, 2001

Triclinic C_{60}·2ferrocene, which melts peritectically at 495 K ($\Delta_\pi H = +50$ J g^{-1}), can form by direct union of its components with a negative excess volume of −68 Å^3 per formula unit, although the enthalpy of deferrocenation into fcc C_{60} and ferrocene vapor is virtually the same as for the sublimation of pure ferrocene. C_{60} solubility in molten ferrocene is about 0.5 mol % at 495 K. The strong anisotropy of the thermal expansion tensor illustrates the anisotropy of intermolecular interactions inferred from the crystal structure in the 90−300 K range. The existence of nonnegligible interactions is corroborated by the persistence of the crystalline local order in the amorphous phase obtained by grinding, which reverts to the initial crystalline phase upon heating. Thus, from the thermodynamic and structural points of view, C_{60}·2ferrocene behaves as the C_{60}·2S_8 solvate.

Introduction

Molecular disorder in pure face-centered cubic C_{60} crystals[1−6] at room temperature is the sole example that almost complies with the Pauling-Fowler model[7,8] according to which molecules freely rotate in their crystalline sites. The space group changes through a first-order phase transition[6] from fcc $Fm\bar{3}m$[9] to simple cubic $Pa\bar{3}$[10,11] at 260 K. Within this new lattice, the molecules undergo orientational motions around two different directions.[12]

Whether and how these disorders are still present in C_{60} solvates in which IR spectroscopy shows almost no,[13] weak,[14] or some[15] charge-transfer remains to be an-

* To whomcorrespondence should be addressed. Telephone: 34 93 401 65 64. Fax : 34 93 401 18 39. E-mail: jose.luis.tamarit@upc.es.

† Permanent address: Laboratoire de Chimie Physique, Faculté de Pharmacie, Université Paris 5, 4 avenue de l'Observatoire, 75006 Paris, France.

(1) Yannoni, C. S.; Johnson, R. D.; Meijer, G.; Bethune, D. S.; Salem, J. R. *J. Phys. Chem*. **1991**, *95*, 9.

(2) Tycko, R.; Haddon, R. C.; Dabbagh, J.; Glarum, S. H.; Douglas, D. C.; Mujsce, A. M. *J. Phys. Chem*. **1991**, *95*, 518.

(3) Tycko, R.; Dabbagh, J. ; Flehming, R. M.; Haddon, R. C.; Makhija, A. V.; Zahurak, S. M. *Phys. Rev. Lett*. **1991**, *67*, 1886.

(4) Johnson, R. D.; Yannoni, C. S.; Dorn, H. C.; Salem, J. R.; Bethune, D. S. *Science* **1992**, *255*, 1235.

(5) Neumann, D. A.; Copley, J. R. D.; Cappelletti, R. L.; Kamitakahara, W. A.; Lindstrom, R. M.; Creegan, K. M.; Cox, D. M.; Romanow, W. J.; Coustel, N.; McCauley, J. P., Jr.; Maliszewskyj, N. C.; Fischer, J. E.; Smith III, A. B. *Phys. Rev. Lett*. **1991**, *67*, 3808.

(6) Heiney, P. A.; Fischer, J. E.; McGhie, A. R.; Romanow, W. J., Jr.; Denenstein, A. M.; McCauley, J. P., Jr.; Smith, A. B., III; Cox, D. E. *Phys. Rev. Lett*. **1991**, *66*, 2911.

(7) Pauling, L. *Phys. Rev*. **1930**, *36*, 430.

(8) Fowler, R. H. *Proc. R. Soc.* **1935**, *149*, 1.

(9) André, D.; Dworkin, A.; Szwarc, H.; Céolin, R.; Agafonov, V.; Fabre, C.; Rassat, A.; Straver, L.; Bernier, P.; Zahab, A. *Mol. Phys*. **1992**, *76*, 1311.

(10) Sachidanandam, R.; Harris, A. B. *Phys. Rev. Lett*. **1991**, *67*, 1467.

(11) Bürgi, H. B.; Blanc, E.; Schwarzenbach, D.; Liu, S. Z.; Lu, Y. J.; Kappes, M. M.; Ibers, J. A. *Angew. Chem., Int. Ed. Engl.* **1992**, *31*, 640.

(12) David, W. I. F.; Ibberson, R. M.; Dennis, T. J. S.; Hare, J. P.; Prassides, K. *Europhys. Lett*. **1992**, *18*, 735.

(13) Kamarás, K.; Hadjiev, V. G.; Thomsen, C.; Pekker, S.; Fodor-Csorba, K.; Faigel, G.; Tegze, M. *Synth. Met*. **1993**, *55*−*57*, 3021.

(14) Semkin, V. N.; Spitsina, N.G; Graja, A. *Chem. Phys. Lett*. **1995**, *233*, 291.

10.1021/cm011171l CCC: $22.00
Published on Web 12/14/2001

swered. Unsuccessful attempts to locate each atom in the unit cells of these solvates at room temperature are related to large amplitude motions of C_{60} molecules that still persist in the solvate crystals.[16−18] However, a two-position orientational disorder of C_{60} was found to account for the crystal structure of the C_{60}·4 benzene solvate at 104 K.[19]

Only two solvate structures, those of C_{60}·$2S_8$[20,21] and C_{60}·2ferrocene,[22] were solved at 298 K by determining and refining the coordinates of individual C-atoms, as if the C_{60} molecules were motionless. In addition, solid-state studies of C_{60}·$2S_8$[23,24] resulted in rather paradoxical conclusions: although this solvate forms with a negative excess volume and local order persists after mechanical amorphization (both results indicating "strong" intermolecular interactions), sulfur was found to behave as if it were free from interactions with C_{60} molecules. Moreover, ^{13}C NMR studies showed that C_{60} molecules in the monoclinic C_{60}·$2S_8$ crystals undergo large amplitude motions around two or more axes.[25] Preliminary NMR experiments[26−28] at room temperature showed that the C_{60} molecules undergo fast reorientational motions also within the C_{60}·2ferrocene solvate and suggested that "the ferrocene mobility becomes much higher in C_{60}·2ferrocene due to the extreme mobility of the surrounding fullerenes". It was even said that "the change in ferrocene mobility ... in comparison with the pure ferrocene can be estimated ... as a factor of 70".[26]

This paper presents solid-state studies on the C_{60} + ferrocene system and on the C_{60}·2ferrocene solvate. The purpose was to characterize them and to compare the results with data previously reported on the C_{60} + sulfur system.[23,24] In particular, it had to be checked to determine whether the triclinic C_{60}·2ferrocene solvate, crystallized from benzene solutions of both components at room temperature,[22] could form directly from solutions of C_{60} in molten ferrocene, and whether other solvates existed in the C_{60} + ferrocene system. In addition, it had to be observed for possible phase transitions at about 260 and 295 K in C_{60}·2ferrocene, as suggested from previous DSC experiments,[28] although the crystal structure was found to be the same at 143 and 296 K.[22]

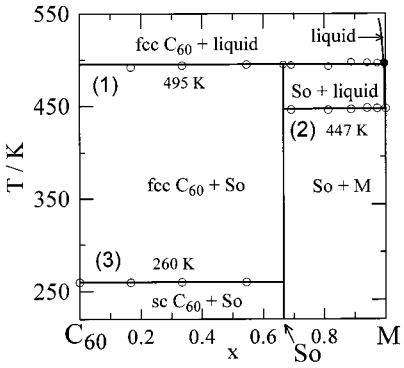

Figure 1. $T-x$ phase diagram of the C_{60} + ferrocene system. So = triclinic C_{60}·2ferrocene, M = monoclinic ferrocene, x = mole fraction of ferrocene, ● = peritectic liquid.

Experimental Section

Sample Preparation. Fcc C_{60} purchased from TermUSA (purity > 99.98%) was used as such and ferrocene ($C_{10}H_{10}Fe$) from Lancaster (purity: 98%) was sublimed before use.

One-hundred-milligram aliquots of C_{60}·2ferrocene solvate were prepared by mixing both components in the C_{60}/ferrocene = 1/2 molar ratio in silica tubes sealed under a 10^{-5}-Torr vacuum. These samples were heated to 458 K, annealed during 15 days at this temperature, and then slowly allowed to cool (during 2 days or so) to room temperature.

Samples for differential scanning calorimetry (DSC) studies were prepared by mixing different proportions of C_{60}·2ferrocene and C_{60} or ferrocene in SETARAM high-pressure stainless steel pans (30-μL inner volume) which were as fully filled as possible (the sample masses were about 23 mg) in order to reduce the sublimation of ferrocene to a minimum. These samples were annealed during 15 days at 423 K and slowly cooled to room temperature within a few days.

Techniques. High-resolution X-ray powder diffraction measurements (Debye−Scherrer geometry and transmission mode) were performed using the CuKα_1 (λ = 1.5406 Å) radiation by means of two INEL CPS-120 diffractometers, working with 0.9 and 1.2 kW power, respectively. The latter was equipped with an OSMIC reflecting mirror in the incident beam and with an INEL cooling device working in the 90−300 K range. To prevent samples from possible shear stress-induced decomposition,[29] they underwent only gentle crushing before being introduced into 0.5-mm diameter Lindemann capillaries. For sample examinations long exposure time ranges (up to 12 h) were used because of X-ray absorption by Fe atoms.

DSC and thermogravimetry (TG) were performed at a 5 K min^{-1} rate under a nitrogen flux with a DSC-10 cell and a TGA-50 balance of a TA2000 T.A.-Instruments thermal analyzer, respectively. Preliminary DSC experiments were performed in the 210−320 K range using a T.A.-Instruments cooling accessory. Sample masses were weighed by means of a 0.01-mg sensitive microbalance. A differential scanning calorimeter (MCB calorimeter, ARION) was also used for measuring sublimation enthalpies at a 1 K min^{-1} rate.

Results

Phase Diagram. The $T-x$ phase diagram shown in Figure 1 was obtained by plotting the onset temperatures of the endothermic effects recorded on heating as a function of the ferrocene mole fraction (x).

(15) Swietlik, R.; Byszewski, P.; Kowalska, E. *Chem. Phys. Lett.* **1996**, *254*, 73.
(16) Maniwa, Y.; Mizoguchi, K; Kume, K.; Kikuchi, K.; Ikemoto, I.; Suzuki, S.; Achiba, Y. *Solid State Commun.* **1991**, *80*, 609.
(17) Pekker, S.; Faigel, G.; Fodor-Csorba, K.; Gránásy, L.; Jakab. E.; Tegze, M. *Solid State Commun.* **1992**, *83*, 423.
(18) Oszlányi, G.; Bortel, G.; Faigel, G.; Pekker, S.; Tegze, M. *Solid State Commun.* **1994**, *89*, 417.
(19) Balch, A. L.; Lee, J. W.; Noll, B. C.; Olmstead, M. M. *J. Chem. Soc., Chem. Commun.* **1993**, 56.
(20) Roth, G.; Adelmann, P. *Appl. Phys. A* **1993**, 169.
(21) Buravov, L. I.; D'yachenko, O. A.; Konovalikhin, S. V.; Kushch, N. D.; Lavrent'ev, I. P.; Spitsyna, N. G.; Shilov, G. V.; Yagubskii, E. B. *Russ. Chem. Bull.* **1994**, *43*, 240.
(22) Crane, J. D.; Hitchcock, P. B.; Kroto, H. W.; Taylor, R.; Walton, D. R. M. *J. Chem. Soc., Chem. Commun.* **1992**, 1764.
(23) Gardette, M.-F.; Chilouet, A.; Toscani, S.; Allouchi, H.; Agafonov, V.; Rouland, J.-C.; Szwarc, H.; Céolin, R. *Chem. Phys. Lett.* **1999**, *306*, 149.
(24) Allouchi, H.; López, D. O.; Gardette, M.-F.; Tamarit, J. Ll.; Agafonov, V.; Szwarc, H.; Céolin, R. *Chem. Phys. Lett.* **2000**, *317*, 40.
(25) Grell, A.-S.; Masin, F.; Céolin, R.; Gardette, M.-F.; Szwarc, H. *Phys. Rev. B*, **2000**, *62*, 3722.
(26) Shabanova, E.; Schaumburg, K.; Kamounah, F. S. *Can. J. Anal. Sci. Spectrosc.* **1998**, *43*, 53.
(27) Vertes, A.; Klencsar, Z.; Kuzmann, E.; Gal, M. *Magyar Kemiai Folyoirat* **1999**, *105*, 10.
(28) Birkett, P. R.; Kordatos, K.; Crane, J. D.; Herber, R. H. *J. Phys. Chem. B* **1997**, *101*, 8975.
(29) Oszlányi, G.; Bortel, G.; Faigel, G.; Pekker, S.; Tegze, M.; Cernik, R. J. *Phys. Rev. B* **1993**, *48*, 7682.

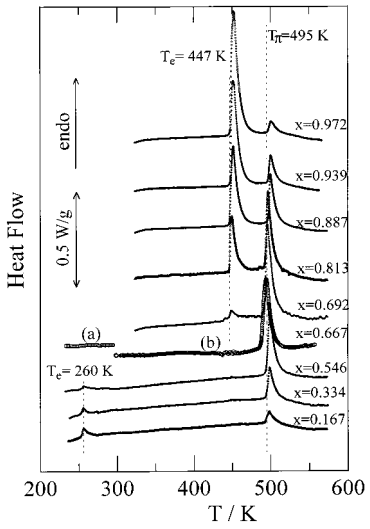

Figure 2. DSC curves on heating binary samples (23.3−24.8 mg) in stainless steel high-pressure pans (30-μL inner volume). The bold curve corresponds to C_{60}·2ferrocene: (a) heating from 213 to 303 K, (b) heating from 298 to 553 K.

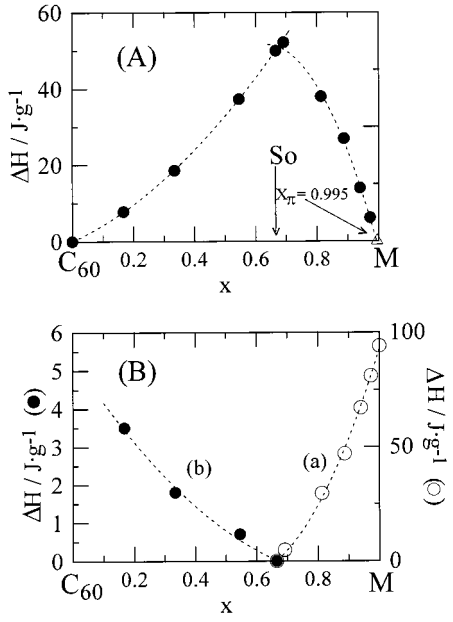

Figure 3. Tammann curves. Enthalpy changes (ΔH) in J g^{-1} as a function of mole fraction x for (A) peritectic equilibrium at 495 K (x_π = mole fraction of the peritectic liquid); (B) curve a = eutectic equilibrium at 447 K, curve b = eutectoid equilibrium at 260 K.

The endothermic peak observed at 495 ± 2 K in the whole composition range (Figure 2), is assigned to the peritectic behavior of a binary compound. Its stoichiometry (C_{60}/ferrocene = 1/2) is determined by drawing the Tammann curve (Figure 3A) associated with the peritectic equilibrium (horizontal line (1) in Figure 1). The composition of the peritectic liquid is found to be $x_\pi = 0.995$ by extrapolating the right-hand part of the Tammann curve to $\Delta H = 0$. The enthalpy change $\Delta_\pi H$ for the C_{60}·2ferrocene peritectic melting was determined to be 50 J g^{-1} (54.6 kJ mol^{-1}, M(C_{60}·2ferrocene) = 1092 g mol^{-1}) at the crossing point of the two branches of the Tammann curve (Figure 3A).

The endothermic peak observed at 447 ± 1 K in the $0.666 < x = 1$ range (Figure 2) is assigned to a eutectic

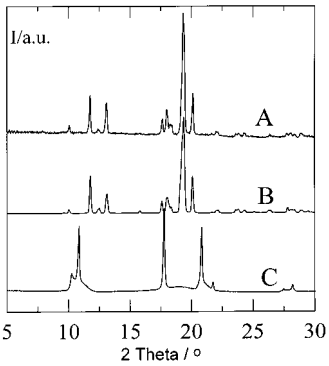

Figure 4. Room-temperature high-resolution X-ray powder diffraction profiles. Experimental (A) and calculated (B) profiles for triclinic C_{60}·2ferrocene. C = C_{60} powder after deferrocenation of C_{60}·2ferrocene.

equilibrium (line (2) in Figure 1) between the C_{60}·2ferrocene solvate and pure ferrocene (T_{fus} = 447 K[30]). An enthalpy change value of 92.3 J g^{-1} was found by extrapolating the related Tammann curve (curve (a) in Figure 3B) to $x = 1$. This is very close to the value (94 J g^{-1} at 447 K) for the melting enthalpy of pure ferrocene encapsulated in high-pressure DSC pans. These results account for the degeneracy of the eutectic equilibrium that precludes the solubility value at this temperature to be estimated. Now assuming that the ferrocene mole fraction of the eutectic liquid is at least equal to that of the peritectic liquid, a eutectic temperature of 446.5 K is calculated according to the Schröder equation.

Another endothermic effect occurs at 260 ± 1 K in the C_{60}-side part of the diagram (line (3) in Figure 1). It is assigned to a eutectoid equilibrium between C_{60} and C_{60}·2ferrocene. The related Tammann curve corresponds to curve (b) in Figure 3B. Extrapolating x to $\Delta H = 0$, a value of 0.667, i.e. the mole fraction for C_{60}·2ferrocene, is found.

No effect, which would allow part of the liquidus curve to be drawn in the ferrocene-rich side of the diagram, was recorded at $T > 495$ K. This indicates that the liquidus curve is probably very steep, as tentatively drawn in Figure 1.

Thermal Stability and Deferrocenation of C_{60}·2Ferrocene. Powders of pure C_{60}·2ferrocene synthesized by direct mixing of its components are made of grains whose shapes are reminiscent of the morphologies of the initial C_{60} crystals. Nevertheless X-ray characterization and DSC experiments revealed no excess of either C_{60} or ferrocene in the solvate powders. Their high-resolution X-ray diffraction profile at 298 K is virtually the same as the one calculated using the atom coordinates for triclinic C_{60}·2ferrocene at room temperature,[22] as shown in Figure 4.

Deferrocenation process starts at about 400−420 K on heating at 5 K min^{-1}. The one-step weight losses (30−36%) found from TG experiments (Figure 5) are close to the ideal value (34.1%). An enthalpy change of 120−150 J per gram of solvate (i.e. 65.5−82.0 J per mole of ferrocene) was found for deferrocenation by integrating the related endothermic effects within the range suggested by the TG curves. This is close to the

(30) Tomassetti, M.; Curini, R.; D'Ascenzo, G.; Ortaggi, G. *Thermochim. Acta* **1991**, *48*, 333.

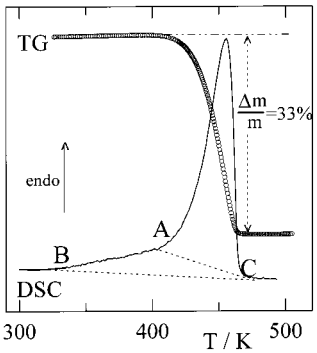

Figure 5. DSC and TG curves of C_{60}·2ferrocene in open pans. Sample masses: DSC = 5.84 mg, TG = 6.47 mg. Integrating the DSC peak within the A−C and B−C ranges gives 120 and 150 J g^{-1}, respectively.

sublimation enthalpy values (64.6−84 kJ mol^{-1}) for pure ferrocene in the same temperature range.[31−33] To confirm this result, another experiment was performed, as for C_{60}·$2S_8$:[23] weighed amounts of C_{60}·2ferrocene were placed in sealed silica tubes (≈40 cm long, 0.6 cm diameter) introduced vertically into one of the two cells of the MCB-ARION differential calorimeter. The main part of each tube (≈35 cm) outside the cell remained at room temperature while the sample inside the cell was heated at a 1 K min^{-1} rate. The areas of the endothermic effects recorded while red-brown crystals of ferrocene grew in the middle part of the tubes were equal to the areas recorded on heating the same masses of pure ferrocene.

Room-temperature X-ray diffraction examination of powders after deferrocenation had occurred shows that the process is accompanied with the formation of the fcc C_{60} phase (profile C in Figure 4). This profile exhibits the same features as those recorded from other desolvated solvates[34,35] and related to defects and stacking faults.[36]

Because the crystal structures of C_{60}·2ferrocene at 143 K and room temperatue are the same,[22] X-ray powder diffraction experiments were performed in the 90−293 K range by steps of about 20 K on heating from 90 K in order to determine thermal expansion and to look for possible (unlikely) phase transition(s). The lattice parameters were refined at each temperature (Figure 6) using the "pattern-matching" option of the FULLPROF program.[37] Then refined lattice parameters and unit-cell volume were fitted as a function of temperature by means of a standard least-squares method. Linear equations for these variations are gathered in Table 1.

To examine the anisotropy of the intermolecular interactions, the thermal-expansion tensor was determined by means of the DEFORM program.[38] The lattice deformation, dU, due to temperature variation, dT, is expressed in terms of a second-rank tensor $dU_{ij} = \alpha_{ij}\, dT$, where α_{ij} (K^{-1}) are the coefficients of the thermal-expansion tensor. Figure 7A shows the three-dimensional plot of the thermal-expansion tensor at 283 K in the frame of the principal axes α_1-α_2-α_3, together with the crystallographic axes.

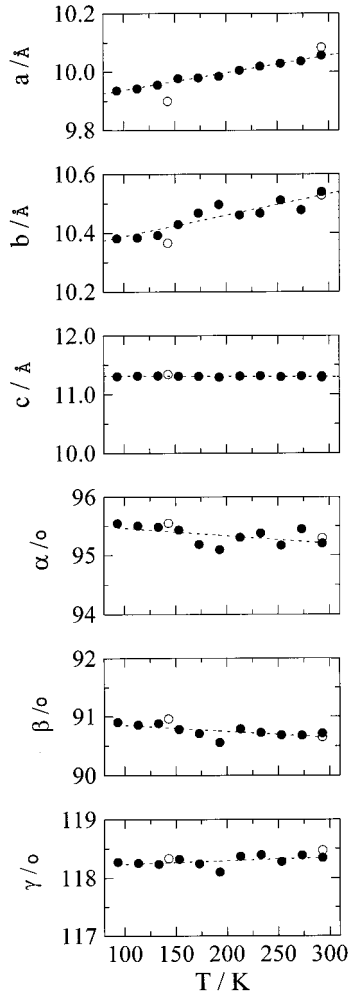

Figure 6. Lattice parameters of triclinic C_{60}·2ferrocene as a function of the temperature. Empty circles correspond to values taken from the crystal structures at 143 and 296 K.[22]

Table 1. Linear Equations $p = p_0 + p_1T$ to Which Lattice Parameters Were Fitted

parameter	P_o/Å	$p_1 \times 10^3$/Å·K^{-1}	$R^a \times 10^4$
a	9.878(4)	0.596(22)	4
b	10.316(22)	0.72(11)	20
c	11.313(7)	−0.024(4)	6
α	95.6(1)	−1.3(6)	13
β	90.93(7)	−0.96(4)	7
γ	118.14(9)	0.46(4)	7

[a] R, defined as $R = \Sigma(y_o - y_c)^2/y_c^2$, is the reliability factor between measured (y_o) and calculated (y_c) lattice constants.

Mechanical Grinding of Triclinic C_{60}·2Ferrocene. For comparison with C_{60}·$2S_8$ solvate, C_{60}·2ferrocene was ground at room temperature using pestle and mortar with increasing grinding times. X-ray powder profiles (Figure 8) of ground powders indicate that the crystal-

(31) Stephenson, R. M.; Malanowski, S. *Handbook of the Thermodynamics of Organic Compounds*; Elsevier: NewYork, 1987.
(32) Beech, G.; Lintonbon, R. M. *Thermochim. Acta* **1971**, *2*, 86.
(33) Kaplan, L.; Kester, W. L.; Katz, J. J. *J. Am. Chem. Soc.* **1952**, *74*, 5531.
(34) Michaud, F.; Barrio, M.; Toscani, S.; López, D. O.; Tamarit, J. Ll.; Agafonov, V.; Szwarc, H.; Céolin, R. *Phys. Rev. B* **1998**, *57*, 10351.
(35) Michaud, F.; Barrio, M.; López, D. O.; Tamarit, J. Ll.; Agafonov, V.; Toscani, S.; Szwarc, H.; Céolin, R. *Chem. Mater.* **2000**, *12*, 3595.
(36) Vaughan, G. B. M.; Chabre, Y.; Dubois, D. *Europhys. Lett.* **1995**, *31*, 525.
(37) Rodríguez-Carvajal, J. *FULLPROF*, a program for Rietveld refinement and pattern matching analyses: Abstracts of the satellite meeting on powder diffraction of the XV[th] congress of the International Union of Crystallography, Toulouse, France, 1990.
(38) Filhol, A.; Lajzerowicz, J.; Thomas, M. *DEFORM* program, unpublished software, 1987.

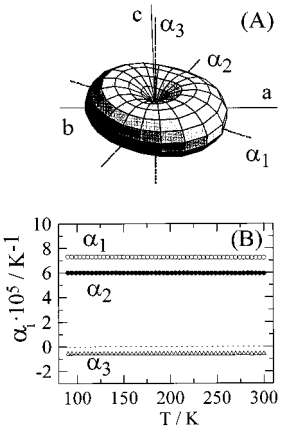

Figure 7. (A) Thermal-expansion tensor of triclinic C_{60}·2ferrocene at 283 K in the frame of the pricipal directions α_1, α_2, α_3 (dashed lines) together with the crystallographic axes (continuous lines). The full length of the α_i axes corresponds to 2×10^{-4} K^{-1}. (B) α_i (i = 1, 2, 3) principal coefficients as a function of the temperature for triclinic C_{60}·2ferrocene.

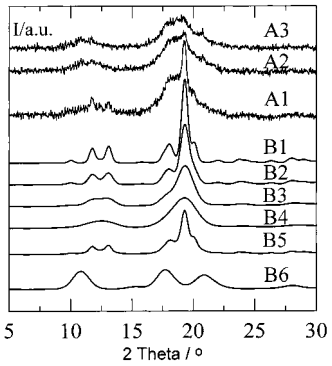

Figure 8. Experimental X-ray profiles of triclinic C_{60}·2ferrocene as a function of the grinding time: A1 = 30 min, A2 = 60 min, A3 = 90 min. Calculated X-ray profiles of triclinic C_{60}·2ferrocene as a function of the crystallite size: B1 = 150 Å, B2 = 100 Å, B3 = 60 Å, B4 = 40 Å, B5 = calculated profile for a mixture of 40-Å (30%) and 150-Å (70%) crystallite sizes, B6 = calculated profile for a mixture of fcc C_{60} and monoclinic ferrocene with a 50-Å crystallite size.

line sample transforms into a noncrystalline (nc) phase within 90 min or so. The DSC curve (Figure 9) of the nc phase obtained after a 90-min grinding exhibits an exothermic effect (peak a) at 453 K (onset) associated with an enthalpy change of about -37.5 J g^{-1} while heating at a 5 K min^{-1} rate. It is followed by an endothermic peak (b) at 489 K (onset) reminiscent of the peritectic melting of the triclinic solvate, as confirmed by the X-ray diffraction at room temperature of the sample recovered at the end of the run. It should be noticed that this profile revealed the presence of some fcc C_{60} besides triclinic C_{60}·2ferrocene. This indicates that the solvate partially dissociates into fcc C_{60} and ferrocene vapor on heating. A possible explanation is that the sample volume (1.2 μL) is small with respect to the inner volume (30 μL) of the high-pressure DSC pan, which can then be saturated with the sample vapor (i.e. almost pure ferrocene). This may explain why the enthalpy value from peak b in Figure 9 is found to be half (25.3 J g^{-1}) that obtained when samples practically fill the inner volumes of the DSC pans (50 J g^{-1}). Indeed, an incomplete transformation of the non crystalline phase might also explain these results.

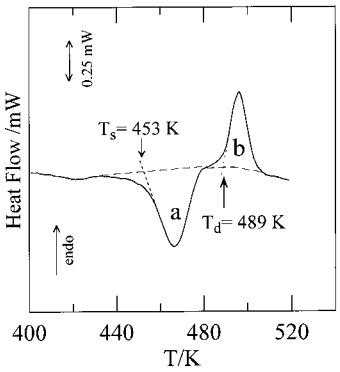

Figure 9. DSC curve obtained on heating a C_{60}·2ferrocene sample previously subjected to a 90-min grinding.

Discussion

The C_{60}·2ferrocene solvate, the sole molecular binary compound found in the C_{60} + ferrocene system, was shown to form from molten ferrocene, as C_{60}·$2S_8$ does from molten sulfur,[23] although the C_{60} solubility in both components is very low (ca. 0.005 mole per mole of solution at 450 K).

The volume of the triclinic C_{60}·2ferrocene at 296 K is 1048 $Å^3$ per formula unit.[22] Assuming a molecular volume of 710 $Å^3$ per C_{60} molecule, as in the fcc unit-cell (a = 14.16 Å), about 338 $Å^3$ remain available for the two ferrocene molecules. If it is assumed that a ferrocene molecule occupies a volume of 203 $Å^3$ per ferrocene molecule, as it does in the ferrocene monoclinic unit-cell,[39] the C_{60}·2ferrocene triclinic solvate forms with a negative excess volume of -68 $Å^3$ per formula unit.

Virtually the same excess volume is found at 143 K taking V/Z = 1017 $Å^3$ [22] for triclinic C_{60}·2ferrocene, V = 698 $Å^3$ per C_{60} molecule, as in the sc unit-cell (a = 14.08 Å at 143 K), and V/Z = 193 $Å^3$ and 196 $Å^3$ at 149 K for orthorhombic and triclinic ferrocene, respectively.[40,41] A linear extrapolation of the ferrocene available volumes (338 $Å^3$ at 296 K and 319 $Å^3$ at 143 K per 2 molecules) to 0 K gives a 301 $Å^3$ volume that hits the calculated van der Waals volume (2 × 149 $Å^3$) for two ferrocene molecules. Now assuming a van der Waals volume of 524 $Å^3$ for a C_{60} "sphere" with 5 Å radius, the packing coefficient for C_{60}·2ferrocene is 0.785 at 296 K and 0.808 at 143 K. Linearly extrapolating the unit-cell volume of C_{60}·2ferrocene to 0 K gives 988 $Å^3$ and a packing coefficient as high as 0.83. Moreover calculating the volume occupied in the triclinic unit-cell by a C_{60} molecule at 0 K (i.e. by subtracting (298 or 301 $Å^3$) from 988 $Å^3$), a value of 687 or 690 $Å^3$ is found, which is the close to that extrapolated to 0 K for the hexagonal polymorph of C_{60} (682 $Å^3$).[42]

To sum up, a negative excess volume and a high packing coefficient allow "strong" interactions between C_{60} and ferrocene molecules to be inferred from crystallographic data, as found previously for a number of C_{60} solvates.[43]

(39) Seiler, P.; Dunitz, J. D. *Acta Crystallogr.* **1979**, *B35*, 2020.
(40) Seiler, P.; Dunitz, J. D. *Acta Crystallogr.* **1982**, *B38*, 1741.
(41) Seiler, P.; Dunitz, J. D. *Acta Crystallogr.* **1979**, *B35*, 1068.
(42) Céolin, R.; Tamarit J. Ll.; López, D. O.; Barrio, M.; Agafonov, V.; Allouchi, H.; Moussa, F.; Szwarc, H. *Chem. Phys. Lett.* **1999**, *314*, 21.

The molecular packing in triclinic C_{60}·2ferrocene (a = 10.084 Å, b = 10.528 Å, c = 11.306 Å, α = 95.29°, β = 90.65°, γ = 118.47° at 296 K[22]), made of alternating C_{60} and ferrocene layers, may be considered as resulting from a distortion of a simple hexagonal packing like that in C_{60}·x I_2[44] or C_{60}·2 CCl_4.[45] Thus, ferrocene molecules are intercalated between dense C_{60} planes at an angle with respect to their own reticular planes. Moreover, the 5-fold axes of the ferrocene molecules are nearly parallel to direction **u v w** = 3 6 $\bar{4}$, as one 5-fold axis of every C_{60} molecule is.

In the triclinic lattice, 2 × 5 shortest C···H(−C) distances (<3.1 Å), i.e. the "strongest" intermolecular interactions, are found to link any C_{60} molecule and its surrounding ferrocene molecules nearly along the 0 1 1 direction, thus resulting in an increased values of angle α with respect to the ideal hexagonal packing. Nevertheless 2 × 16 supplementary C···H(−C) distances in the 3.1−3.5 Å range yield interactions which, as a whole, are roughly perpendicular to C_{60} and ferrocene layers.

This is illustrated by the shape of the thermal expansion tensor (Figure 7A) whose α_3 direction, the "hard direction" along which strong interactions operate, is nearly perpendicular to molecular layers, i.e. nearly parallel to axis c. In addition, the "soft" α_1 and α_2 directions, whose coefficients are close to each other, lie in a plane parallel to plane ab, i.e. to homo-molecular layers. Data in Figure 7B show that this picture of the C_{60}−ferrocene interactions does not depend on temperatures in the 90−300 K range.

Transformation of triclinic C_{60}·2ferrocene into a noncrystalline phase upon grinding further supports the previous inferences for the existence of "strong" interactions between C_{60} and ferrocene molecules. The experimental profiles recorded after increasing grinding-time ranges were compared with those calculated by decreasing the crystallite size to 40 Å (Figure 8). It can be seen that the 90-min profile is similar to the 40-Å profile, although a small contribution of the mixture of pure components with a 50-Å particle size (profile B6 in Figure 8) cannot be discarded. In addition, the 30-min profile can result from the contribution of various crystallite sizes. Although the structure does not survive grinding, as proven by the exothermic recrystallization of the amorphous phase (peak a in Figure 9), the agreement between experimental and calculated profiles indicates that the local order of the triclinic phase is retained in the noncrystalline phase and resists grinding.

Nevertheless, the deferrocenation enthalpy was found to be equal to the sublimation enthalpy of pure ferrocene, thus suggesting that no extra-interaction between C_{60} and solvating molecules takes place on forming solvates.

Concluding Remarks

The phase-diagram method brings basic and reliable information to the binary compounds it reveals. As far as C_{60}·2ferrocene is concerned, it showed that no crystal−crystal phase transition occurs in the 90−495 K range. This disagrees with previous DSC measurements which revealed two endothermic peaks at 260 and 295 K (onsets), respectively,[28] although the crystal structures were found to be the same at 143 K and at 296 K.[22] Thus the chemical identity of the sample previously examined through Mossbauer spectroscopy remains elusive.

Although ^{13}C NMR studies have shown that intermolecular interactions do not prevent C_{60} molecules from undergoing large amplitude motions within the monoclinic C_{60}·2S_8 crystals, it was possible to ascribe their motionless appearance, from the crystallographic point of view, to jumps between equivalent (symmetry-related) molecular orientations, probably because molecular symmetry axes are very close to reticular axes.[25] In the case of C_{60}·2ferrocene, NMR studies have already shown that the C_{60} molecules undergo fast reorientational motions, whereas the ferrocene molecules move more slowly if they move at all.[26] Future dynamic studies should answer this question. Another question to be answered arises from the near parallelism between the 5-fold axes of ferrocene molecules and a 5-fold axis of every C_{60} molecule. It remains to be established whether there is some coupling between the possible motions of both kinds of molecules around their respective 5-fold axes: NMR studies as a function of temperature should shed some light on this problem.

Acknowledgment. Grant PB98-0923 (DGES, Spain) and the Banque Nationale de Belgique are acknowledged for this work performed under INTAS-RFBR Contract 97-1015. One of us (R.C.) is grateful for an invited position from the Generalitat de Catalunya at the Universitat Politècnica de Catalunya and financial support from BIOCODEX Lab., France (Dr. J. Vincent).

CM011171L

(43) Céolin, R.; Michaud, F.; Toscani, S.; Agafonov, V.; Tamarit, J. Ll.; Dworkin A.; Szwarc, H. In *Recent Advances in the Chemistry and Physics of Fullerenes and Related Materials*; Kadish, K. M., Ruoff, R. S., Eds.; The Electrochemical Society: Pennington, NJ, 1997; Vol. 5, p 373.

(44) Zhu, Q.; Cox, D. E.; Fischer, J. E.; Kniaz, K.; McGhie, A. R.; Zhou, O. *Nature* **1992**, *355*, 712.

(45) Keita, B.; Nadjo, L.; Céolin, R.; Agafonov, V.; André, D.; Szwarc, H.; Dugué, J.; Fabre, C.; Rassat A. *Chem. Phys.* **1994**, *179*, 595.